ELSEVIER

Journal of Nuclear Materials 276 (2000) 59–64

journal of nuclear materials

www.elsevier.nl/locate/jnucmat

Kinetic Monte Carlo studies of the effects of Burgers vector changes on the reaction kinetics of one-dimensionally gliding interstitial clusters

H.L. Heinisch[a,*], B.N. Singh[b], S.I. Golubov[b,1]

[a] *Pacific Northwest National Laboratory, P.O. Box 999, MS P8-15, Richland, WA 99352, USA*[2]
[b] *Materials Research Department, Risø National Laboratory, DK-4000 Roskilde, Denmark*

Abstract

Kinetic Monte Carlo simulations of one-dimensionally diffusing interstitial clusters (dislocation loops) are used to gain insight into their role in microstructure evolution under irradiation. The simulations investigate the changes in reaction kinetics of these defects as a function of changes in the Burgers vector and variation in the size and density of randomly or periodically distributed sinks. In this paper we report on several kinetic Monte Carlo studies intended to elucidate the effects of mixed 1-D/3-D migration relative to pure 3-D and pure 1-D migration. We have investigated the effects of variation of the average distance traveled between Burgers vector changes $\langle L \rangle$ on the absorption of individual defects into absorbers of varying size and varying concentration, as well as the effects of variation in $\langle L \rangle$ on the time dependence of absorption of a collection of defects into an array of absorbers. Significant effects of Burgers vector changes on the reaction kinetics of the diffusing interstitial clusters are clearly demonstrated. Even when $\langle L \rangle$ is large relative to the size and spacing of microstructural features, significant effects of mixed 1-D/3-D migration on reaction kinetics are evident.

1. Introduction

A comparison of the available experimental results on cluster density and void swelling clearly demonstrates that there are very significant differences in the defect accumulation behavior between fcc and bcc metals irradiated under cascade damage conditions over a wide temperature range [1]. In an attempt to understand the mechanisms responsible for causing these large differences in the swelling behavior between fcc and bcc metals, Golubov, Singh and Trinkaus, in a companion article to this [2], have analyzed the experimental results on void swelling within the framework of the production bias model (PBM) with the assumption of one-dimensional (1-D) diffusional transport of self-interstitial atom (SIA) clusters. Molecular dynamics (MD) studies have demonstrated that SIA produced in cascades can readily take the configuration of crowdions and crowdion clusters that migrate one-dimensionally. Furthermore, they have shown that the structure, stability, and the fraction of glissile SIA clusters that are produced in cascades in bcc iron are different from that in fcc copper [3,4].

The concept of 'pure' 1-D diffusional transport implies that the gliding SIA clusters, which are essentially small glissile dislocation loops, maintain the same Burgers vector throughout their lifetime, i.e., until they interact with a sink. Recently, it was found that incorporating the assumption of pure 1-D diffusional transport of SIA clusters into the PBM does not provide an adequate explanation for the observed large differences

* Corresponding author. Tel.: +1-509 376 3278; fax: +1-509 376 0418.
E-mail address: hl_heinisch@pnl.gov (H.L. Heinisch)

[1] Permanent address: Institute of Physics and Power Engineering, Bondarenko Sq. 1, 249020 Obninsk, Russian Federation.

[2] Pacific Northwest National Laboratory is operated for the US Department of Energy by Battelle Memorial Institute under contract DE-AC06-76RLO 1830.

0022-3115/00/$ - see front matter
PII: S0022-3115(99)00169-5

in the swelling behavior between fcc and bcc metals [2]. Rather, Golubov et al. [2] have proposed that the treatment of the damage accumulation in the PBM should include the effects of changes in the Burgers vector of SIA clusters during their 1-D diffusional transport. MD simulation studies have shown that such changes can occur either by thermal activation [5,6] or by interaction with another SIA cluster [7]. The net effect of this kind of migration is a defect migration path that is 3-D but consists of segments of 1-D random walks. The concept of mixed 1-D/3-D migration is illustrated (in 2-D sketches) in Fig. 1(c), where the average length between direction changes, $\langle L \rangle$, is proportional to the square root of the average number of 1-D jumps made between direction changes. The reaction kinetics of this mixed 1-D/3-D type of migration will depend on the average length of 1-D segments relative to the size and concentration of other defects and microstructural features with which the SIAs can interact.

The reaction kinetics for pure 3-D diffusion and pure 1-D diffusion can be formulated analytically. Unfortunately, at present, there exists no rigorous mathematical description of the reaction kinetics for 1-D glide with random Burgers vector changes, leading to the mixed 1-D/3-D mode of diffusional transport. However, some guidance can be found from earlier work by Gösele and Seeger [8], who analytically described the reaction kinetics of single crowdions involved in defect recovery during annealing experiments. In this work they considered 'preferentially' 1-D migration, in which 1-D migrating crowdions jump infrequently from one row of atoms to another as they continue in the same direction, as illustrated schematically in Fig. 1(d). Their work demonstrated that even a very small deviation from the pure 1-D diffusion (in preferentially 1-D migration) leads to a decisive change in the reaction kinetics. While this conclusion of Gösele and Seeger has been taken to be the central argument in the treatment of defect accumulation and void lattice formation in fcc and bcc metals by Golubov et al. [2], there still remains the difficulty of analytically describing the effects of random Burgers vector changes and mixed 1-D/3-D migration.

To gain insight into these processes, we have begun using kinetic Monte Carlo simulations of one-dimensionally diffusing SIA clusters to investigate the changes in reaction kinetics as a function of changes in the Burgers vector and variation in the size, R, and concentration (number density), C, of randomly or periodically distributed sinks.

In this paper we report on several kinetic Monte Carlo studies intended to elucidate the effects of mixed 1-D/3-D migration relative to pure 3-D and pure 1-D migration. In particular we have investigated the effects of the number of jumps, N (or the average distance traveled, $\langle L \rangle$) between Burgers vector changes on the absorption of individual defects into absorbers of

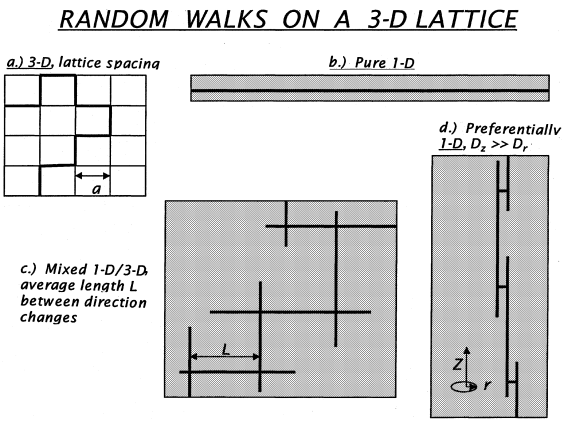

Fig. 1. Schematic illustration of defect migration by (a) 3-D random walk on the crystal lattice; (b) 1-D random walk; (c) mixed 1-D/3-D migration consisting of a 3-D path consisting of segments of 1-D random walks in different random directions; and (d) preferentially 1-D migration consisting of segments of 1-D random walks in the same direction broken by occasional hops to adjacent atom rows.

varying size and varying concentration, as well as the effects of variation in $\langle L \rangle$ on the time dependence of absorption of a collection of defects into an array of absorbers.

2. Procedure

Empirical computational studies of the effects of mixed 1-D/3-D migration and the scale of the microstructure on defect reaction kinetics were performed using a simple kinetic Monte Carlo computer code, following the basic concepts of the ALSOME kinetic Monte Carlo code used for annealing studies of cascades [9] and simulations of defect accumulation under irradiation [10]. In the present study, a defect associated with a site in a fcc lattice migrates by jumping randomly along any of the 12 $\langle 1\,1\,0 \rangle$ directions to a neighboring lattice site. In principle, the defect can represent any type of migrating defect: vacancy, self interstitial atom (dumbbell or crowdion), or clusters thereof, as long as it can be 'associated' spatially with a lattice site, and its migration is effectively from lattice site to lattice site along $\langle 1\,1\,0 \rangle$ directions. In the present work all mobile defects have the same kinetic properties. The mobile defects interact with immobile, spherical 'absorbers' of radius R located within the volume. A migrating defect is absorbed into an absorber when their center-to-center separation is less than R. The mobile defects do not interact among themselves.

All defects migrate by jumping one $\langle 1\,1\,0 \rangle$ lattice vector at a time. A defect migrating by 'pure 3-D' mi-

gration chooses its next jump randomly from all 12 possible ⟨1 1 0⟩ jump vectors, as illustrated schematically in Fig. 1(a). A defect migrating by 'pure 1-D' migration chooses its next jump randomly from either plus or minus directions along the same ⟨1 1 0⟩ direction, Fig. 1(b).

In these simulations a defect performing mixed 1-D/3-D migration jumps back and forth in a 1-D random walk along the same ⟨1 1 0⟩ direction for N jumps, then a new direction for its next 1-D random walk segment is chosen randomly from the 12 ⟨1 1 0⟩ directions. It proceeds with this 1-D random walk for another N jumps, and so on, Fig. 1(c). In the simulations discussed here N is taken to have the same value for each 1-D segment of the mixed 1-D/3-D migration for a given run. To keep the discussion in terms of varying length scales, we characterize the mixed 1-D/3-D path by the average length $\langle L \rangle$ between direction changes (since in our simulations N has the same value for each 1-D segment, we shall drop the 'average' notation $\langle L \rangle$ and refer from now on to $L = a(N/2)^{1/2}$, where a is the fcc lattice parameter, as the average distance between direction changes). Note, however, that the total length of the actual 1-D path traversed during a specific 1-D segment can be greater than L.

In the present study, the absorbers are stationary and unsaturable, and they are arranged in either random or periodic arrangements in computational cells of finite size depending on the problem studied. A simple cubic periodic arrangement of absorbers is accomplished by placing one absorber at the center of the cell and imposing periodic boundaries at the cell faces. Thus, the spacing between absorbers and their concentration C is determined by the size of the cell. A computation volume of finite size is simulated by requiring the defect to be absorbed in the boundary after it has completely traversed the cell volume a fixed number of times. A random arrangement of absorbers is simulated by placing absorbers at random locations within a very large cell.

Absorption at the boundary represents a second absorber population in competition with the array of spherical absorbers distributed within the computational volume. The results of these studies are likely to be quantitatively different if a secondary absorber of different size (absorption at the boundary of larger or smaller computational volume) or different geometry is used. However, qualitatively, the same relative behavior in defect absorption with respect to changes in L, R or C is expected. Moreover, by having the boundary as the secondary absorber, the interplay of the effects of varying L, R and C may be more clearly demonstrated.

3. Results

Several studies were undertaken using the Monte Carlo approach outlined above. The independent variable in most cases was the number of jumps N between direction changes, varying from $N = 1$ for pure 3-D migration with equally probable jumps along any of the 12 ⟨1 1 0⟩ directions to $N = \infty$ for pure 1-D migration. Most figures are plotted here in terms of the average distance between direction changes, L, in order to consider the effects of this length variable relative to the various other length scales. Lengths are shown in the figures in units of nm, assuming the fcc lattice parameter in these studies to be that of Cu, about 0.36 nm. In the results shown here, each data point represents the average value for a set of 1000 mobile defects, each initiated at a random position within the central region of the computational cell and with randomly chosen initial migration directions.

In Fig. 2 the fraction of defects absorbed by a periodic array of static absorbers is plotted as a function of L for absorbers of six different radii. Each absorber is at the center of a cubic cell of size 100 lattice parameters (about 36 nm for fcc Cu), resulting in an absorber concentration of about $2 \times 10^{22}/\mathrm{m}^3$. The total computational volume is a cube containing 125 such cells in a periodic array. The absorber radii are varied from 1% to 25% of the cell size. The 1000 migrating defects are initiated one at a time in the central cell, and the fraction of these that are absorbed before they can escape the computational volume is plotted for each value of L and R considered. In Fig. 2 the values for $L = \infty$ (pure 1-D) are plotted at $L = 10^4$ nm. The fraction absorbed under pure 1-D migration can be determined simply from the cross sectional area of the absorber relative to the cross sectional area of the cell in the ⟨1 1 0⟩ direction. The effects of absorber radius can be clearly seen. When the absorbers have smaller radii, a smaller fraction of migrating defects are absorbed at all values of L. Also, the mixed 1-D/3-D reaction kinetics manifest a transition from more 3-D-like to more 1-D-like behavior with

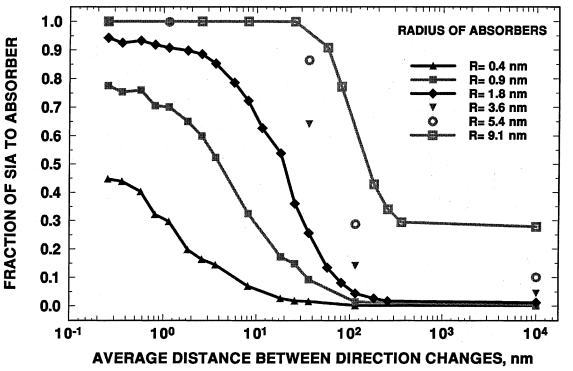

Fig. 2. The fraction of migrating SIA absorbed in a periodic array of absorbers as a function of L, the average distance between direction changes, for fixed concentration, $C = 2 \times 10^{22}/\mathrm{m}^3$, and various values of absorber radius.

increasing L that occurs more sharply as the absorber radius increases. On a relative scale, however, the smaller the absorber, the more sensitive the fraction of absorption is to the value of L.

In Fig. 3 the fraction of defects absorbed by a periodic array of static absorbers is plotted as a function of L for six different levels of concentration of a periodic array of absorbers of radius $R = 0.9$ nm. Conditions are the same as for Fig. 2. As in Fig. 2, when the probability of meeting an absorber increases (in this case because of a higher concentration of absorbers), the transition of the mixed 1-D/3-D kinetics from 1-D-like to 3-D-like behavior as a function of L becomes much sharper. Fig. 4 shows the same information plotted relative to the absorption fractions for pure 1-D. In general, the lower the concentration, the more sensitive the absorption fraction is to the value of L (although the effects of varying the concentration appear to saturate in the $2–4 \times 10^{22}/\mathrm{m}^3$ concentration range). In Fig. 5 the same data are plotted to show the absorption fraction as a function of the absorber density for various values of L. The dependence of absorption fraction on absorber density varies significantly with the value of L.

The studies discussed above were performed on a periodic array of absorbers. For comparison, a problem using a random array of absorbers of radius 0.9 nm was studied. Mobile defects were introduced at random positions in the central region of the cell, and the simulation was carried out as in the studies of the periodic arrays of absorbers. In Fig. 6 the results for the random array are compared to those for the periodic array of absorbers. For this simple set of conditions the results for the random array and the periodic array are the same within the scatter to be expected. However, this may not be true in general, when, for example, more than one type of absorber is present.

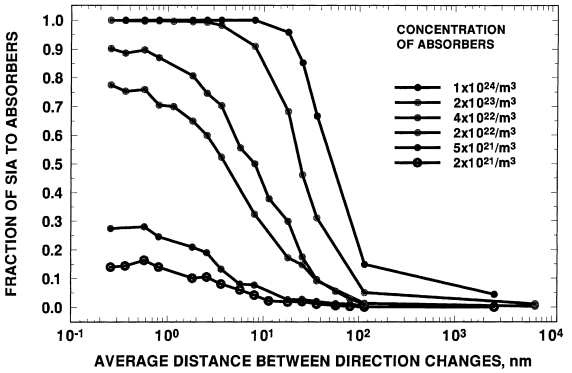

Fig. 3. The fraction of migrating SIA absorbed in a periodic array of absorbers as a function of L, the average distance between direction changes, for absorbers of fixed radius, $R = 0.9$ nm, having various values of concentration.

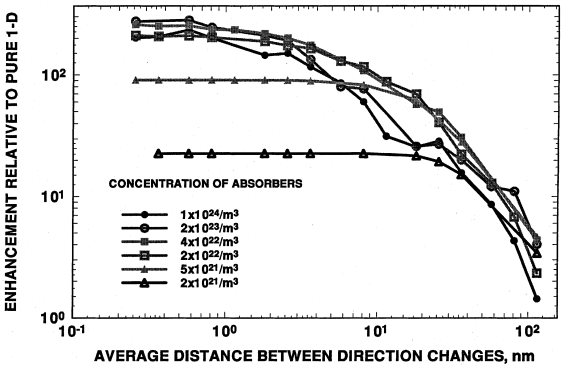

Fig. 4. The fractions, relative to that for pure 1-D migration, of migrating SIA absorbed in a periodic array of absorbers as a function of L, the average distance between direction changes, for absorbers of fixed radius, $R = 0.9$ nm, having various values of concentration.

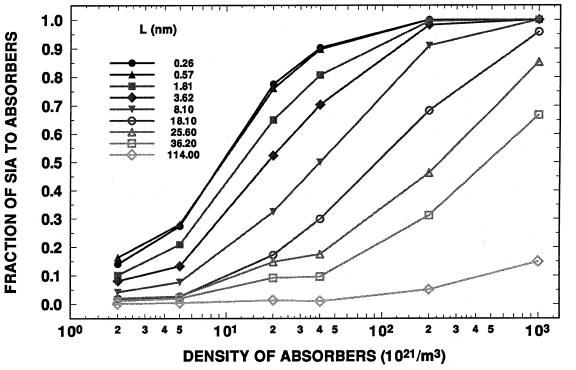

Fig. 5. The fraction of migrating SIA absorbed in a periodic array of absorbers of fixed radius, $R = 0.9$ nm, as a function of the concentration of absorbers, for various values of L, the average distance between direction changes.

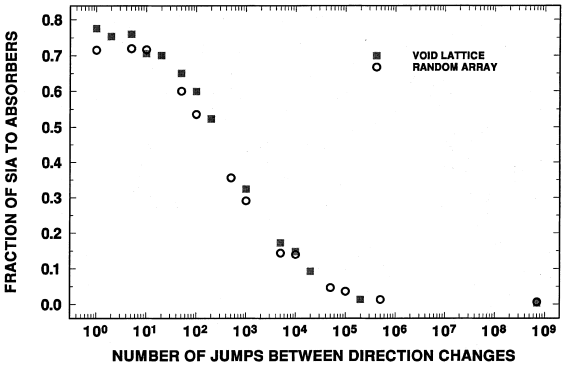

Fig. 6. The fraction of migrating SIA absorbed as a function of L, the average distance between direction changes, for a periodic array of absorbers of fixed radius, $R = 0.9$ nm, and concentration, $C = 4 \times 10^{22}/\mathrm{m}^3$, and a random array of absorbers of the same size and average spacing.

To further elucidate the effects of mixed 1-D/3-D migration on defect reaction kinetics, a simulation was performed to simulate recovery of damage (or decay of a defect population) as a function of time. In this case 1000 defects were placed randomly and simultaneously in a cubic cell of side 100 nm. containing a random array of spherical absorbers at a concentration of $1 \times 10^{22}/m^3$. The absorbers were static and unsaturable, and they were maintained at a constant radius of 2.4 nm (6.5 lattice parameters in Cu) throughout the recovery runs. The mobile defects jumped randomly on the fcc lattice, and they did not interact with each other. Infinite periodic boundaries were applied, and defects were absorbed only by the spherical absorbers. Each run was terminated after a fixed number of jumps for the system. Figs. 7 and 8 show the number of defects absorbed in the absorbers as a function of time, which is measured in units of defect jumps. The log–log plot in Fig. 7 emphasizes the differences in the curves at small values. Results are shown for runs using various values of L. The upper curve is for 3-D migration. The lower curve is for pure 1-D ($L = \infty$), and it tends toward a saturation value reflecting the finite size of the periodic cell. In between are plotted results for values of $L = 25$, 36, 57, 81, 116 and 181 nm. For each of the intermediate values of L, the system follows the trace for the pure 1-D case (the same set of random numbers is used in all cases) until it deviates to a trace more similar to that of the 3-D migration, although at a lower slope with increasing L (Fig. 8). In every intermediate case, there is a transition from 1-D behavior to mixed 1-D/3-D behavior once the defects have migrated distances comparable to the distances between direction changes. In all cases shown in Figs. 7 and 8 the fraction absorbed at the transition to mixed kinetics is about 3% or less, which is, of course, the value of absorption under pure 1-D migration.

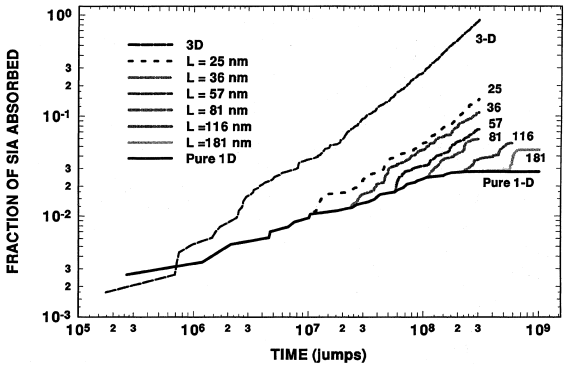

Fig. 7. The fraction of SIA absorbed as a function of time from an initial concentration of mobile SIA $10^{24}/m^3$, randomly distributed near the center of a random array of stationary spherical absorbers of concentration, $C = 10^{22}/m^3$, and radius, $R = 2.5$ nm for various values of L, the average distance between direction changes.

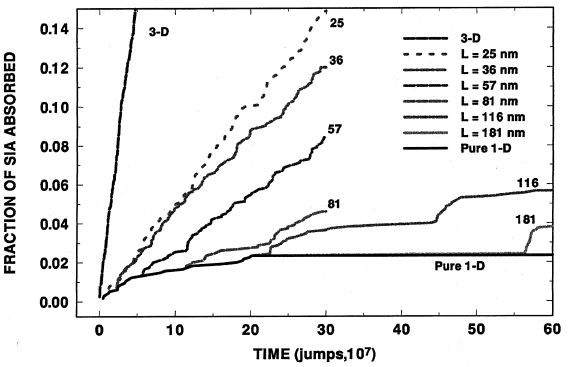

Fig. 8. A linear plot of Fig. 7. The fraction of SIA absorbed as a function of time from an initial concentration of mobile SIA $10^{24}/m^3$, randomly distributed near the center of a random array of stationary spherical absorbers of concentration, $C = 10^{22}/m^3$, and radius, $R = 2.5$ nm for various values of L, the average distance between direction changes.

4. Discussion and conclusions

The studies described here illustrate how defect reaction kinetics change when mixed 1-D/3-D defect migration takes place due to dislocation loops (clustered crowdions) gliding one-dimensionally with frequent or occasional changes in their Burgers vectors. This suggests that when evaluating the magnitude of damage accumulation under cascade damage conditions, it is important to consider not only 1-D diffusion of SIA clusters, but especially to consider also the effects of changes in the Burgers vector on the reaction kinetics of these clusters with the sinks in the crystal.

The change in defect reaction kinetics depends on L, the average distance between Burgers vector direction changes in the mixed 1-D/3-D migration paths of the defects, relative to the scale of the microstructure with which the defects interact. There are obviously scale extremes where the defect migration is essentially pure 1-D or 3-D. If the Burgers vector changes after only a few hops on average, then its migration is essentially 3-D. If L is equal to or larger than the grain size, the migration is essentially 1-D. However, Figs. 7 and 8 illustrate that even when L becomes large relative to the spacing of potential interaction partners, there is always a regime in which mixed 1-D/3-D reaction kinetics will be operable. Also, given that mean free paths are longer under 1-D migration than under 3-D, the mixed 1-D/3-D kinetics will likely dominate.

In a global sense the reaction kinetics can change during continuous irradiation as the scale of the microstructure changes through defect accumulation and microstructure evolution. The present results indicate that the way the kinetics change during microstructure evolution depends on the value of L. Referring to Fig. 5, it can be expected that in an actual irradiation the

density of absorbers (immobile defect clusters – dislocation loops, stacking fault tetrahedra, etc.) will increase with dose and that, during that transient period, the reaction kinetics of defects diffusing by mixed 1-D/3-D migration will change differently with the defect cluster density for different values of L. Furthermore, since the Burgers vector changes may be strongly influenced by local interactions with defects, it is likely that L will also change with increasing dose. This makes the dependence of the reaction kinetics on the frequency of change of the Burgers vector for defects undergoing mixed 1-D/3-D migration very complicated.

The present study has revealed the complicated nature of the defect reaction kinetics of gliding interstitial loops that diffuse by mixed 1-D/3-D migration. The profound effects of this phenomenon will only be realized when we obtain sufficient understanding to include it in global theories of microstructure evolution under neutron irradiation.

Acknowledgements

The authors gratefully acknowledge A.J.E. Foreman for his interest in this work and his valuable comments on the manuscript. This work was partly supported by the US Department of Energy under contract DE-AC06-76RLO 1830 with Battelle Memorial Institute a the Pacific Northwest National Laboratory and partly supported by the European Fusion Technology Programme.

References

[1] B.N. Singh, J.H. Evans, J. Nucl. Mater. 226 (1995) 277.
[2] S.I. Golubov, B.N. Singh, H. Trinkaus, these Proceedings, p. 78.
[3] Yu. N. Osetsky, V. Priego, A. Serra, B.N. Singh, S.I. Golubov, Philos. Mag. A, in press.
[4] Yu. N. Osetsky, V. Priego, A. Serra, B.N. Singh, S.I. Golubov, Philos. Mag. A, submitted.
[5] N. Soneda, T. Diaz de la Rubia, Philos. Mag., in press.
[6] F. Gao, D.J. Bacon, Yu. N. Osetsky, P.E.J. Flewitt, T.A. Lewis, these Proceedings, p. 213.
[7] Yu.N. Osetsky, A. Serra, V. Priego, these Proceedings, p. 202.
[8] U. Gösele, A. Seeger, Philos. Mag. 34 (1976) 177.
[9] H.L. Heinisch, B.N. Singh, J. Nucl. Mater. 251 (1997) 77.
[10] H.L. Heinisch, B.N. Singh, J. Nucl. Mater. 271&272 (1999) 46.